Atmos. Chem. Phys., 13, 12073–12088, 2013
www.atmos-chem-phys.net/13/12073/2013/
doi:10.5194/acp-13-12073-2013

Atmospheric Chemistry and Physics Open Access

Analyzing experimental data and model parameters: implications for predictions of SOA using chemical transport models

K. C. Barsanti[1], **A. G. Carlton**[2], **and S. H. Chung**[3]

[1]Department of Civil & Environmental Engineering, Portland State University, Portland, Oregon
[2]Department of Environmental Sciences, Rutgers University, New Brunswick, New Jersey
[3]Department of Civil & Environmental Engineering, Washington State University, Pullman, Washington

Correspondence to: K. C. Barsanti (barsanti@pdx.edu)

Received: 10 May 2013 – Published in Atmos. Chem. Phys. Discuss.: 14 June 2013
Revised: 19 October 2013 – Accepted: 23 October 2013 – Published: 13 December 2013

Abstract. Despite critical importance for air quality and climate predictions, accurate representation of secondary organic aerosol (SOA) formation remains elusive. An essential addition to the ongoing discussion of improving model predictions is an acknowledgement of the linkages between experimental conditions, parameter optimization and model output, as well as the linkage between empirically-derived partitioning parameters and the physicochemical properties of SOA they represent in models. In this work, a "best available" set of SOA modeling parameters is selected by comparing predicted SOA yields and mass concentrations with observed yields and mass concentrations from a comprehensive list of published smog chamber studies. Evaluated SOA model parameters include existing parameters for two product (2p) and volatility basis set (VBS) modeling frameworks, and new 2p-VBS parameters; 2p-VBS parameters are developed to exploit advantages of the VBS approach within the computationally-economical and widely-used 2p framework. Fine particulate matter ($PM_{2.5}$) and SOA mass concentrations are simulated for the continental United States using CMAQv.4.7.1; results are compared for a base case (with default CMAQ parameters) and two best available parameter cases to illustrate the high- and low-NO_x limits of biogenic SOA formation from monoterpenes. Results are discussed in terms of implications for current chemical transport model simulations and recommendations are provided for future modeling and measurement efforts. The comparisons of SOA yield predictions with data from 22 published chamber studies illustrate that: (1) SOA yields for naphthalene, and cyclic and >C5 straight-chain/branched alkanes are not well represented using either the newly developed or existing parameters for low-yield aromatics and lumped alkanes, respectively; and (2) for four of seven volatile organic compound+oxidant systems, the 2p-VBS parameters better represent chamber data than do the default CMAQ v.4.7.1 parameters. Using the "best available" parameters (combination of published 2p and newly derived 2p-VBS), predicted SOA mass and $PM_{2.5}$ concentrations increase by up to 15 % and 7 %, respectively, for the high-NO_x case and up to 215 % ($\sim 3\,\mu g\,m^{-3}$) and 55 %, respectively, for the low-NO_x case. Percent bias between model-based and observationally-based secondary organic carbon (SOC) improved from −63 % for the base case to −15 % for the low-NO_x case. The ability to robustly assign "best available" parameters in all volatile organic compound+oxidant systems, however, is critically limited due to insufficient data; particularly for photo-oxidation of diverse monoterpenes, sesquiterpenes, and alkanes under a range of atmospherically relevant conditions.

1 Introduction

Atmospheric fine particulate matter ($PM_{2.5}$) has long been linked to direct climate forcing, with estimates of radiative forcing due to the sulfate fraction surpassing that due to the organic carbon fraction (Haywood and Boucher, 2000 and references therein). However, more recently, Goldstein et al. (2009) reported that for the southeastern United States (US) the spatial and temporal distributions of aerosol optical thickness (AOT) are most consistent with biogenic organic aerosol precursors (e.g., α-pinene), suggesting secondary

organic aerosol (SOA) can dominate AOT in the summer, affecting negative radiative forcing or cooling in the region. A modeling study by Myhre et al. (2009) also suggests that SOA is a significant contributor to negative radiative forcing, on a global scale. Additional radiative forcing (Park et al., 2010), though positive in sign, may be possible if one considers the production of brown carbon from SOA constituents (Updyke et al., 2012). SOA, by virtue of its contribution to $PM_{2.5}$ (20–50 % globally, Hallquist et al., 2009), also plays a role in adversely affecting health (e.g., Pope, 2007). It is thus of critical importance that a quantitative and predictive understanding of SOA be achieved. To that end, much effort has been directed at developing, improving, and testing SOA models that are sufficiently comprehensive yet not computationally burdensome.

Accurate representation of SOA is elusive, even at the process-level, and becomes increasingly so as attempts are made to simplify and parameterize systems that are not fully understood. While the focus of this work is on bottom-up SOA modeling approaches, top-down approaches exist as well (e.g., Spracklen et al., 2011). One bottom-up approach to simulating SOA in three-dimensional chemical transport models (CTMs) proceeds by combining anthropogenic and biogenic emissions estimates with smog chamber data on SOA formation from individual volatile organic compound (VOC) precursors to generate regional and/or global SOA fields (Hallquist et al., 2009). Representation of SOA formation is based on gas/particle (G/P) partitioning theory (Pankow, 1994a, b) and historically parameterized using the two-product (2p) approach of Odum et al. (1996), in which up to two lumped products are assumed to represent the condensable oxidation products of each VOC+oxidant system. For each such system, products are assigned empirically-derived partitioning parameters (K_p or C^*) and stoichiometric product yields (α) using a least-squares fitting approach, typically such that one product has a relatively lower α value and lower volatility (product 1) and the other has a relatively higher α value and higher volatility (product 2). An alternative, more recent approach is the volatility basis set (VBS) approach (Donahue et al., 2006; Lane et al., 2008b), in which C^* values are defined by fixed logarithmically-spaced bins and least-squares fitting is used to assign α values (e.g., Pathak et al., 2007a). In addition to SOA formation from oxidation of volatile precursors ("traditional" SOA), the VBS approach has been used to parameterize SOA formation based on smog chamber studies of intermediate to low volatility precursors (Grieshop et al., 2009; Presto et al., 2010), including those precursors produced from the evaporation of primary organic aerosol (POA) (Grieshop et al., 2009).

While there are a variety of limitations associated with using smog chamber data to derive model parameters to represent SOA formation in the real atmosphere (e.g., Kroll and Seinfeld, 2008), and more detailed modeling approaches are being developed (e.g., GECKO-A, Aumont et al., 2005; Lee-Taylor et al., 2011; and CNPG, Pankow and Barsanti, 2009; Barsanti et al., 2011), most widely-used approaches for predicting SOA in CTMs rely on parameterizations of chamber experiments. These CTMs include CAM-Chem (Lack et al., 2004; Heald et al., 2008), CMAQ (Carlton et al., 2010), GEOS-Chem (Henze and Seinfeld, 2006; Pye et al., 2010), GISS GCM (Chung and Seinfeld, 2002) and PM-CAMx (Lane et al., 2008b; Tsimpidi et al., 2011). The default implementation of the 2p and VBS approaches in these CTMs, as well as the fitting of 2p and VBS parameters, assumes instantaneous G/P equilibrium. Recent work suggests that this assumption is appropriate in CTMs (Saleh et al., 2013), though other recent studies (Virtanen et al., 2010; Cappa and Wilson, 2011; Vaden et al., 2011; Perraud et al., 2012; Shiraiwa and Seinfeld, 2012) suggest that this assumption may not be appropriate under all conditions; changes in the physicochemical properties of particles due to ambient condition changes and/or condensed-phase chemistry may lead to circumstances where partitioning kinetics are controlled by particle-phase diffusion. In this work, the default assumption of instantaneous equilibrium is retained.

Chamber studies conducted with very high initial precursor concentrations (and subsequently high reacted hydrocarbon levels, ΔHC), lead to very high organic aerosol mass concentrations (M_o) relative to ambient values. Because high M_o values favor SOA condensation, even relatively volatile compounds can contribute significantly to the SOA that forms. In dark α-pinene ozonolysis experiments by Yu et al. (1999) $\sim$ 50–95 % of the SOA mass formed can be attributed to identified and hypothesized oxidation products that are relatively volatile, with K_p values on the order of 10^{-6} to 10^{-1} m^3 µg^{-1} ($C^* \approx 10^5$ to 10 µg m^{-3}). In more recent dark α-pinene ozonolysis experiments by Camredon et al. (2010), also at high M_o, all of the proposed and identified major monomeric oxidation products in the condensed phase have K_p values on the order of 10^{-5} to 10^{-1} m^3 µg^{-1} ($C^* \approx 10^4$ to 10 µg m^{-3}). However, only products at the lowest end of such volatility distributions ($K_p = 10^{-1}$ m^3 µg^{-1} or $C^* = 10$ µg m^{-3}) would be expected to condense at an atmospherically relevant M_o of ~ 5 µg m^{-3}, and for those products, only $\sim$ 33 % would be expected in the condensed phase.

When the 2p fitting approach is applied to chamber data from experiments carried out at high ΔHC levels (and thus high M_o), the relatively volatile products with higher stoichiometric yields (α) form in significant levels, "masking" the presence of lower volatility products with much lower α values. Thus, while lower volatility products do not influence K_p values derived from high M_o chamber experiments, such products may explain most of the SOA formation in the atmosphere. Evidence for this has been provided by low M_o chamber experiments (Presto and Donahue, 2006; Pathak et al., 2007a; Shilling et al., 2008). As described in Presto and Donahue (2006), the VBS fitting approach has some advantages over the 2p fitting approach that are achieved by fixing the volatility bins (C^* values) based on experimental and/or

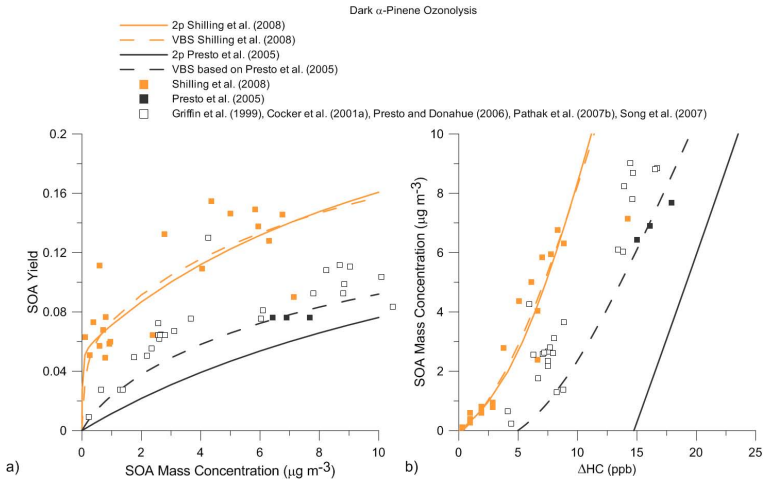

Fig. 1. Comparison of 2p (solid lines) and VBS (dashed lines) parameterizations for dark α-pinene ozonolysis chamber experiments, as influenced by the range in SOA mass concentration and number of data points at low SOA mass concentration. **(a)** SOA yield vs. SOA mass concentration; **(b)** SOA mass concentration vs. level of reacted hydrocarbon (ΔHC).

ambient M_o ranges and fitting only the α values. For a typical 4-species basis set (e.g., $C^* = \{1, 10, 100, 1000\}$ μg m^{-3}) the number of free parameters, four, is the same as with the 2p approach; however, the VBS parameters are much less covariant because the volatility space is fixed. Furthermore, because of the fixed logarithmically-spaced volatility bins, VBS parameters may be better able to represent SOA formation at low M_o, specifically when limited data exist. In this work, parameters based on VBS fits are developed and evaluated in an effort to take advantage of the robustness of the VBS fitting approach within the computationally economical, precursor specific, and widely used 2p modeling framework. These new parameters are herein called "2p-VBS".

Principles of G/P partitioning theory are used here to guide a detailed analysis of the often overlooked, but non-trivial linkages between experimental conditions, parameter optimization, and predictions of SOA using CTMs. A detailed comparison of predicted SOA yields and mass concentrations using the 2p, VBS, and the new 2p-VBS parameters with published smog chamber data is conducted and used to recommend the "best" parameters based on currently available data. The "best available" parameters then are used in CMAQ to simulate SOA and $PM_{2.5}$ over the continental US during a two-week summer period. Results of the analysis and model predictions are used to highlight current knowledge gaps and may be used to guide future chamber experiments and SOA modeling efforts.

2 Approach

2.1 Development of 2p-VBS parameters

In this section, the motivation and approach for developing the new 2p-VBS parameters are described. Figure 1a and b illustrate the relationship between chamber M_o and ΔHC levels and predicted SOA yields and mass concentrations using 2p and VBS fitting approaches for dark α-pinene ozonolysis experiments (shown only for $M_o \leq 10$ μg m^{-3}, see Supplement Table S1 for a descriptive list of all of the experimental data considered, including full M_o and ΔHC ranges). As introduced above, the SOA fitting parameters are influenced both by the range in M_o, as well as the number of data points at low M_o. The Presto et al. (2005) data spans ΔHC levels from 15–210 ppb and M_o values from 7–346 μg m^{-3} (three data points with $M_o < 10$ μg m^{-3}), while Shilling et al. (2008) spans ΔHC levels from 0.3–14 ppb and M_o from 0.1–7 μg m^{-3} (twenty data points with $M_o < 10$ μg m^{-3}). Results from Shilling et al. (2008) suggest that when sufficient data points were available at low M_o both the 2p and VBS parameterizations represented the observed yields (Fig. 1a) and captured the observed SOA formation at the lowest ΔHC levels (Fig. 1b). For the Presto et al. (2005) dataset, while the observed yields at $M_o > 50$ μg m^{-3} were represented by the published 2p parameterization (not shown here, see Presto et al., 2005), observed SOA formation at the lowest ΔHC levels (15–25 ppb) was not captured (Fig. 1b). In this work, VBS parameters were fit to the Presto et al. (2005) dataset; the VBS parameters were better able to represent observed SOA formation at ΔHC levels < 25 ppb in the experiments from which the parameters were derived, as well as in other chamber experiments for the same VOC+oxidant system (Griffin et al., 1999; Cocker et al., 2001a; Pathak et al., 2007b; Song et al., 2007). These results suggest that the VBS approach may be better able to represent SOA formation at low ΔHC levels and M_o, specifically when data are available but sparse, due to the fixed logarithmically-spaced volatility bins across the experimentally relevant M_o range. The ability of any individual parameterization to represent SOA formation

will further depend on the quality of data used in the fitting and the chemical similarity between the observed and modeled systems.

In the context of chemical transport modeling, the inability of some chamber-based parameterizations to accurately capture SOA formation at low, atmospherically relevant ΔHC levels has important consequences for spatial and temporal predictions of atmospheric $PM_{2.5}$, as well as implications for analyses of the relative contributions of specific SOA precursors, including source-attribution analyses. Therefore, in an effort to exploit the fitting advantages of the VBS approach and potentially provide improved parameters for use within the 2p modeling framework, 2p-VBS parameters were developed for evaluation as follows. For the traditional SOA precursors, the published VBS parameters of Tsimpidi et al. (2010) at $T = 298$ K were used to generate 263 pseudo-data points (yield vs. M_o) for $M_o = 0$ to 200 μg m^{-3} at each of three temperatures (272, 298, and 324 K) using an effective $\Delta H_{vap} = 30$ kJ mol^{-1} (see Pathak et al. 2007b); those 789 pseudo-data points were then fit to generate a set of 2p-VBS parameters for each set of VBS parameters. The 2p-VBS parameters are presented in Table 1 for $T = 298$ K and $\rho = 1.5$ g cm^{-3} (the same temperature and density reported in Tsimpidi et al. (2010); see Supplement for derivation of the density correction). In addition to the volatile SOA precursors, 2p-VBS parameters were derived for semi-volatile alkanes and POA (Table 2) based on the VBS parameters of Presto et al. (2010), Shrivastava et al. (2008) and Grieshop et al. (2009). Following Shrivastava et al. (2008) in which the effective ΔH_{vap} varied with C^* for POA, here ΔH_{vap} was treated as an additional fitting parameter (values are included in Table 2). Published VBS parameters were chosen as the starting point for this work because of the ability of VBS parameterizations to represent SOA formation over a wide ΔHC and M_o range and the limited availability of validated data within the range of atmospherically relevant ΔHC and M_o.

For each of the traditional SOA precursors, the 2p-VBS parameters reproduced the yield curves from the VBS parameters over the range of M_o data, at each of the three temperatures, and were able to represent SOA formation with the same degree of uncertainty as the VBS parameters (i.e., no additional error is introduced by the 2p-VBS fit, see Supplement Figure S1). Therefore, the SOA yield and mass predictions using the Tsimpidi et al. (2010) VBS parameters and the 2p-VBS parameters derived here produce equivalent results for "first generation" SOA formation, including the temperature dependence of SOA yields. Consequently, only predictions using the 2p-VBS parameters are shown in subsequent figures (i.e., predictions using Tsimpidi et al. (2010) VBS parameters are not shown). Differences between the 2-VBS parameters in this work and the reduced species VBS parameters in Shrivastava et al. (2011), also developed to reduce computational burden, are described in the Supplement (see Fig. S2).

2.2 Chemical transport modeling

CMAQ (Byun and Schere, 2006) version 4.7.1 was used to simulate SOA mass concentrations over the continental US (12 × 12 km resolution) up to 50 mb with 34 vertical layers (4 666 194 grid cells) for 12–31 July 2006. This date range is representative of typical US summertime conditions when biogenic SOA is a measurable component of total $PM_{2.5}$ (Kleindienst et al., 2010). The simulation results for the first three days were excluded from subsequent analysis to allow for model initialization and spin-up. The gas-phase chemistry mechanism SAPRC07 (Carter, 2010) was used for the simulations, with updated isoprene photo-oxidation chemistry to improve isoprene nitrate yields, isoprene nitrate lifetimes, and NO_x recycling rates (Xie et al., 2013). Anthropogenic emissions were based on the 2005 National Emissions Inventory (NEI) projected to 2006; biogenic emissions were generated with the Biogenic Emissions Inventory System (BEIS) model version 3.14. Meteorological inputs for BEIS and pollutant transport were from version 3.1 of the Weather Research Forecasting (WRF) model. Three cases were considered: a base case using the revised CMAQv4.7 parameters (i.e., CMAQv4.7.1 parameters) described in Carlton et al. (2010) and two additional cases exploring best available SOA parameters and sensitivity to NO_x-dependent biogenic SOA formation (BA-highNO_x and BA-lowNO_x). Selection of the best available parameters was based on the comparison of 2p, VBS and 2p-VBS predictions with chamber data, as described in detail in the results and discussion section. The default aging mechanism of CMAQv4.7.1 was retained, wherein traditional SOA is converted to nonvolatile SOA with a rate constant $k_{olig} = 9.6 \times 10^{-6}$ s^{-1} (Carlton et al., 2010).

CMAQv4.7.1 allows NO_x-dependent SOA formation for anthropogenic precursors only (see Carlton et al., 2010); thus two case studies (BA-highNO_x and BA-lowNO_x) were constructed to illustrate the limits of SOA formation from monoterpenes under "high" and "low" NO_x conditions. For the aromatic precursors within CMAQ, the branching between the high- and low-NO_x SOA formation pathways is treated dynamically as a function of the ratio of nitric oxide (NO) to hydroperoxy radical (HO_2) and the reaction rates of the peroxyradical (RO_2) with NO and HO_2 (Henze et al., 2008). Therefore, the anthropogenic high-NO_x parameters were the same in the prescribed BA-highNO_x and BA-lowNO_x case studies, and were selected as described below. For the anthropogenic low-NO_x parameters, the default CMAQv4.7.1 values were used. While legitimate questions exist as to the relationship between NO_x conditions in chambers and NO_x conditions in the real atmosphere (and how each are defined), a detailed investigation is beyond the scope of this manuscript. For biogenic precursors, the division between high- and low-NO_x experimental data and SOA parameterizations was thus based on a number of factors: (1) the designations given in

Table 1. 2p-VBS parameters, based on VBS parameters of Tsimpidi et al. (2010), for SOA precursors under high- and low-NO_x conditions at $T = 298$ K and $\rho = 1.5\,g\,cm^{-3}$.

Precursor	High NO_x					Low NO_x				
	α_1	C_1^*	α_2	C_2^*	Data Sources	α_1	C_1^*	α_2	C_2^*	Data Sources
ALK4	0.038	10				0.075	10			
ALK5	0.150	10			a, b, c	0.300	10			
OLE1	0.009	9.0	0.116	284		0.014	4.0	0.170	236	
OLE2	0.032	8.1	0.216	244		0.055	2.8	0.297	170	
ARO1 = TOL	0.186	10	0.488	180		0.218	3.2	0.625	103	d, e
ARO2 = XYL	0.219	11	0.487	185	d	0.275	3.7	0.639	97	
ISO	0.020	7.4	0.018	68	f	0.019	2.1	0.032	28	
TERP	0.130	7.3	0.433	191		0.160	1.7	0.615	126	
SESQ fit for $M_o \leq 30\,\mu g\,m^{-3}$	0.647	18			g, h, i	n/a				

Data sources for the Tsimpidi et al. (2010) parameterizations are provided if specifically discussed in the text. [a] Wang et al. (1992); [b] Takekawa et al. (2003); [c] Lim and Ziemann (2005); [d] Ng et al. (2007b); [e] Hildebrandt et al. (2009); [f] Pandis et al. (1991); [g] Hoffmann et al. (1997); [h] Griffin et al. (1999); [i] Ng et al. (2007a).

Table 2. 2p-VBS parameters based on VBS parameters for alkanes (Presto et al., 2010), naphthalene (Pye et al., 2010), undifferentiated POA (Shrivastava et al., 2008), wood smoke POA and diesel POA (Grieshop et al., 2009) under high-NO_x conditions for $T = 298$ K and $\rho = 1.0\,g\,cm^{-3}$.

Precursor	α_1	C_1^*	$\Delta H_{vap,1}$	α_2	C_2^*	$\Delta H_{vap,2}$
$C_{12}H_{26}$	0.091	4.7	30	0.569	218	30
$C_{13}H_{28}$	0.121	1.1	30	0.666	52.6	30
$C_{14}H_{30}$	0.139	0.7	30	0.675	31.4	30
$C_{15}H_{32}$	0.155	0.6	30	0.674	23.4	30
$C_{16}H_{34}$	0.167	0.5	30	0.672	19.0	30
$C_{17}H_{36}$	0.183	0.5	30	0.664	16.0	30
Naphthalene	0.144	2.9	30	0.226	33.7	30
POA	0.257	0.7	112	0.501	180	77
Wood Smoke POA	0.228	1.6	69	0.473	103	56
Diesel POA	0.239	4.4	66	0.479	213	58

the associated publications, (2) reported $HC_{initial}$ / $NO_{x\,initial}$ and/or ΔHC / $NO_{x\,initial}$ ratios, and (3) comparisons among reportedly similar data/parameterizations (see Supplement Table S1 for chamber experiment details). The selection of biogenic SOA parameters, specifically for monoterpenes, under high-NO_x conditions (BA-highNO_x) and low-NO_x conditions (BA-lowNO_x) is described below. The parameters selected for each case are summarized in Table 3.

3 Results and discussion

3.1 Biogenic precursor parameters

In Figs. 2–4, for each of the biogenic precursors (isoprene, monoterpenes, sesquiterpenes), two panels are shown. The first is SOA yield vs. M_o and the second is M_o vs. ΔHC. Theoretical yield (panel a) and SOA (panel b) curves using 2p, VBS, and/or 2p-VBS parameters are shown, along with chamber data. The predicted SOA curves are particularly well-suited for illustrating the ability (or inability) of model parameters to represent SOA formation under ambient conditions. Where sufficient chamber data were available, the figures were limited to $M_o < 10$–$30\,\mu g\,m^{-3}$ to further highlight the atmospherically relevant range. For the precursors that have been more widely studied (e.g., monoterpenes), a subset of published chamber data was selected based either on the use of the data in derivation of CTM model parameters or on the experimental conditions (relatively low/atmospherically relevant ΔHC levels and M_o). Parameters were evaluated for both high- and low-NO_x conditions.

3.1.1 Isoprene parameters

In Fig. 2, the 2p-VBS theoretical yield (Fig. 2a) and SOA formation (Fig. 2b) curves for isoprene are compared with those from two additional parameterizations widely used in chemical transport modeling: (1) the Henze and Seinfeld (2006) low-NO_x 2p parameterization based on the chamber experiments of Kroll et al. (2006), and (2) the high-NO_x "3p" parameterization of Pandis et al. (1991). Also shown are upper-bound (low-NO_x) and lower-bound (high-NO_x) parameterizations from Carlton et al. (2009) (note: the lower-bound parameterization is outside the axis range in Fig. 2b). For the low-NO_x conditions, the 2p-VBS underpredicted SOA yields compared to chamber observations (Fig. 2a) and was not able to reproduce the observed SOA formation at the lowest ΔHC levels (Fig. 2b) (chamber data: Kroll et al., 2005, 2006; Chan et al., 2010; Chhabra et al., 2010). The low-NO_x VBS parameterization, on which the 2p-VBS parameterization was based, relied on extrapolation of chamber data as described in Lane et al. (2008b). Briefly, the high-NO_x VBS parameters

Table 3. Default parameters (base case) and best available parameters for biogenic high NO_x (BA-highNO_x) and biogenic low NO_x (BA-lowNO_x) used in CMAQv4.7.1 simulations[a]; $T = 298$ K and densities[b] matched to reported densities for base case (Carlton et al., 2010). Data references not provided in this work can be found in Carlton et al. (2010) for 2p parameters and in Tsimpidi et al. (2010) for VBS parameters.

	Base Case				Best Available (BA)				
Precursor	α_1	C_1^*	α_2	C_2^*	α_1	C_1^*	α_2	C_2^*	Source
ALK5	0.072	0.02			0.10	6.7			2p-VBS
TOL = ARO1[c]	0.076	2.3	0.148	21.3	0.201	8.5	0.527	149	2p-VBS
XYL = ARO2[c]	0.039	1.3	0.112	34.5	0.039	1.3	0.112	34.5	CMAQ
ISO	0.029	0.6	0.232	116	0.029	0.6	0.232	116	CMAQ
TERP (high NO_x)	0.139	14.8	0.454	134	0.112	6.3	0.376	165	2p-VBS
TERP (low NO_x)	n/a				0.139	1.5	0.533	110	2p-VBS
SQT = SESQ	1.537	25.0			1.537	25.0			CMAQ

[a] NO_x dependent SOA pathways for anthropogenic compounds are treated in CMAQv.4.7.1, with branching calculated as a function of RO_2 reaction with NO vs. HO_2. Only the high NO_x anthropogenic parameters are shown here; the CMAQ default low NO_x anthropogenic parameters were used in all simulations. High NO_x and low NO_x biogenic cases were run to illustrate the limits of SOA production in each of these scenarios (note: only the TERP parameters vary with NO_x level, see text for discussion);
[b] Density, ρ (g cm^{-3}): ALK5, 1.0; TOL, 1.24; XYL, 1.48; ISO, 1.4; TERP, 1.3; SQT, 1.3;
[c] Each α value (CMAQ and 2p-VBS) was divided by 0.765 (TOL) or 0.804 (XYL) to account for a stoichiometric factor in the implementation of the SAPRC mechanism in CMAQv4.7.1.

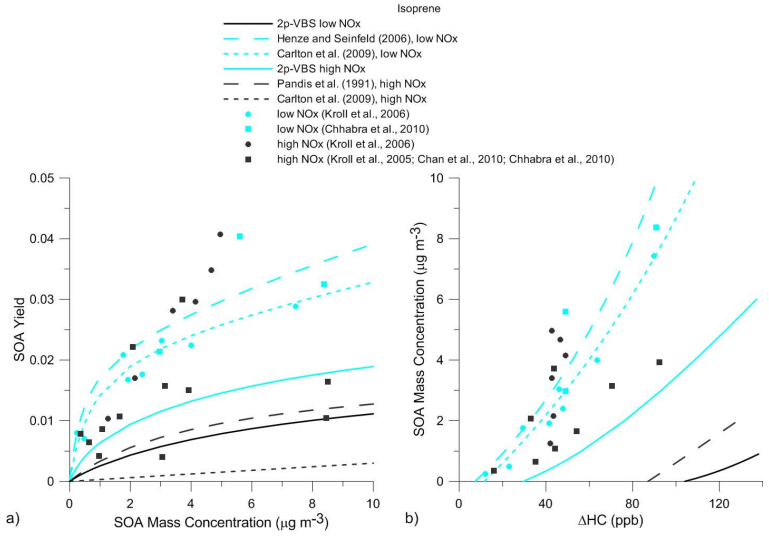

Fig. 2. Evaluation of 2p and 2p-VBS parameterizations for isoprene under low-NO_x (cyan) and high-NO_x (black) conditions. **(a)** Theoretical yield curve (SOA yield vs. SOA mass concentration); **(b)** predicted SOA mass curve (SOA mass concentration vs. level of reacted hydrocarbon, ΔHC).

(Lane et al., 2008a; Tsimpidi et al., 2010), based on the "3p" parameterization of Pandis et al. (1991), were adjusted using an M_o-dependent yield correction from the α-pinene experiments and parameterizations of Pathak et al. (2007a). It is thus not unexpected that the low-NO_x 2p-VBS parameterization was not able to represent observed SOA formation, particularly at the lowest ΔHC levels. In contrast, the low-NO_x 2p parameterizations of Henze and Seinfeld (2006) and of Carlton et al. (2009) were derived directly from chamber data and were in better agreement with the chamber observations (Kroll et al., 2006; Chhabra et al., 2010). The default low-NO_x parameters based on Henze and Seinfeld (2006), which notably produce the highest predicted SOA yields, were retained as the best available parameters for the CMAQ simulations.

There have been limited studies investigating the effects of NO_x on isoprene SOA yields (Carlton et al., 2009 and references therein). The parameterizations shown here suggest that increasing NO_x potentially results in lower SOA yields (Fig. 2a); however, as described by Surratt et al. (2010) and Chan et al. (2010), SOA yields depend on relative concentrations of HO_2, NO and NO_2, complicating the interpretation

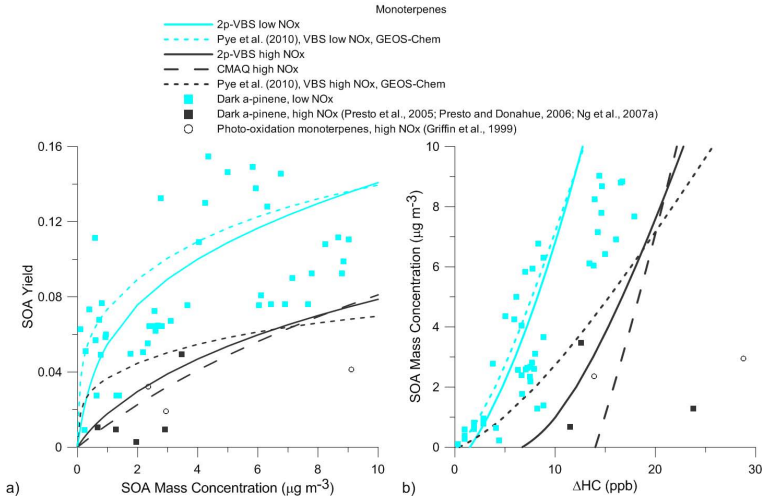

Fig. 3. Evaluation of 2p and 2p-VBS parameterizations for lumped monoterpenes under low-NO_x (cyan) and high-NO_x (black) conditions. **(a)** Theoretical yield curve (SOA yield vs. SOA mass concentration); **(b)** predicted SOA mass curve (SOA mass concentration vs. level of reacted hydrocarbon, ΔHC).

of NO_x dependence. For the high-NO_x isoprene conditions, none of the parameterizations were able to represent the SOA yields (Fig. 2a) or SOA formation observed at the lowest, atmospherically relevant, ΔHC levels (Fig. 2b). NO_x dependence of SOA formation by isoprene was not considered here, given that: (1) under some conditions, highest yields have been observed under high-NO_x conditions when NO_2 / NO ratios are high and RO_2+NO_2 reactions are favored over RO_2+NO reactions (e.g., Chan et al., 2010); and (2) the effects of NO_x on the volatility of the initially formed products (e.g., the point at which SOA formation is observed) are not clear (Fig. 2b).

3.1.2 Monoterpene parameters

In Fig. 3, the 2p-VBS theoretical yield (Fig. 3a) and SOA formation (Fig. 3b) curves for lumped monoterpenes are compared with those obtained from parameterizations used in CMAQv.4.7.1 (Carlton et al., 2010) and GEOS-Chem (Pye et al., 2010). Given the limited data available from photo-oxidation studies of monoterpenes, data also are shown for dark α-pinene ozonolysis chamber experiments (low NO_x referenced in Fig. 1, high NO_x: Presto et al., 2005; Presto and Donahue, 2006; Ng et al., 2007a). As argued by Pye et al. (2010), dark α-pinene ozonolysis parameters may serve as a good proxy for lumped monoterpene photo-oxidation parameters because the parameters derived from dark α-pinene ozonolysis experiments likely overestimate yields from photo-oxidation of α-pinene, but likely underestimate yields from photo-oxidation of other monoterpenes known to have higher yields than α-pinene.

The CMAQ (Carlton et al., 2010) high-NO_x 2p parameters were based on the chamber experiments of Hoffmann et al. (1997) and Griffin et al. (1999); there is no low-NO_x monoterpene SOA formation pathway in CMAQv.4.7.1. In Pye et al. (2010), the low-NO_x VBS parameters were based on dark α-pinene ozonolysis chamber experiments of Shilling et al. (2008). The low-NO_x VBS parameters in Lane et al. (2008b) and Tsimpidi et al. (2010) were calculated as a weighted average for individual monoterpenes based on chamber studies under a range of experimental conditions (e.g., UV vs. dark, high vs. low RH). In Pye et al. (2010) and Lane et al. (2008a) the high-NO_x VBS parameters were extrapolated from the low-NO_x parameters as follows: (1) Pye et al. (2010) applied a fixed yield correction based on the α-pinene experiments of Ng et al. (2007a) and Pathak et al. (2007a), and (2) Lane et al. (2008a) applied a M_o-dependent yield correction based on Pathak et al. (2007a). The lower yields and mass concentrations predicted in this work with the 2p-VBS parameters, relative to those predicted with the Pye et al. (2010) VBS parameters, are a consequence of both the lower observed SOA yields for UV conditions (data used in low-NO_x VBS parameterization) and the greater yield correction in calculating the high-NO_x parameters. Note that while the use of the high-NO_x isoprene VBS parameters (Lane et al., 2008a) to obtain the low-NO_x isoprene parameters leads to a likely underestimation of SOA formation (Fig. 2a), the use of the low-NO_x monoterpene VBS parameters (Lane et al., 2008a; Pye et al., 2010) to obtain the high-NO_x parameters leads to reasonable and perhaps an overestimation of SOA formation (Fig. 3). The high-NO_x monoterpene parameterization of Pye et al. (2010), derived from the low-NO_x Shilling et al. (2008) experiments, appears to overestimate SOA formation at low ΔHC and M_o levels (Fig. 3b). However, the data are insufficient to make robust conclusions regarding the best available parameters, highlighting the need for monoterpene photo-oxidation

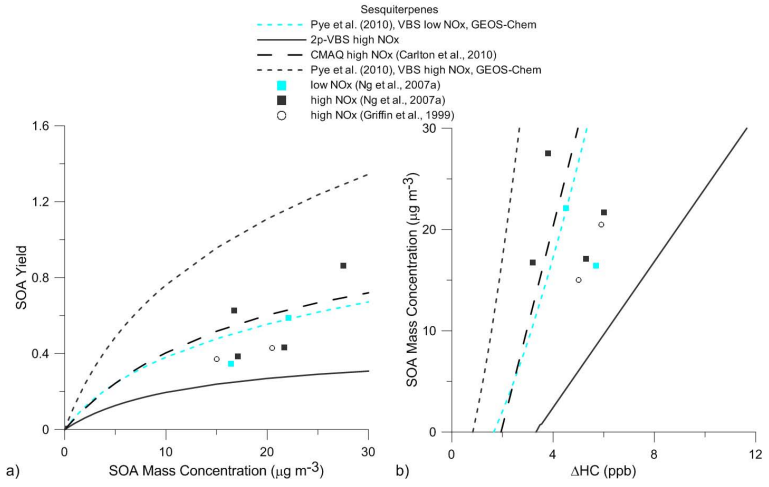

Fig. 4. Evaluation of 2p and 2p-VBS parameterizations for lumped sesquiterpenes under low-NO_x (cyan) and high-NO_x (black) conditions. **(a)** Theoretical yield curve (SOA yield vs. SOA mass concentration); **(b)** predicted SOA mass curve (SOA mass concentration vs. level of reacted hydrocarbon, ΔHC).

studies under varying atmospherically relevant NO_x conditions. Based on the available data, the 2p-VBS parameters for both low- and high-NO_x conditions were chosen for the CMAQ simulations.

3.1.3 Sesquiterpene parameters

In Fig. 4, the 2p-VBS theoretical yield (Fig. 4a) and SOA formation (Fig. 4b) curves for lumped sesquiterpenes are compared with curves from the 2p parameterization used in CMAQv.4.7.1 (Carlton et al., 2010) and the VBS parameterization in GEOS-Chem (Pye et al., 2010). Relative to the 2p and VBS parameterizations, the 2p-VBS parameterization underestimated SOA yields (Fig. 4a) and M_o (Fig. 4b) (chamber data: Griffin et al., 1999; Ng et al., 2007a). The VBS parameters (Lane et al., 2008b; Tsimpidi et al., 2010), on which the 2p-VBS parameters were based, and the CMAQ (Carlton et al., 2010) and Pye et al. (2010) parameters all were derived from chamber experiments involving α-humulene or β-caryophyllene as the sesquiterpene precursor; however, the Lane et al. (2008b)/Tsimpidi et al. (2010) VBS parameters were derived using data from photo-oxidation as well as dark ozonolysis experiments (Ng et al., 2006). For α-humulene and β-caryophyllene, the dark ozonolysis yields were significantly lower than the photo-oxidation yields, which likely resulted in the low bias of the Lane et al. (2008b) parameterization, and thus the low bias of the 2p-VBS parameterization as compared with CMAQ (Carlton et al., 2010) and GEOS-Chem (Pye et al., 2010).

Both the CMAQ (Carlton et al., 2010) and Pye et al. (2010) parameterizations were based on the chamber photo-oxidation data of Griffin et al. (1999), which had ΔHC [ppbC] / $NO_{x\,initial}$ [ppb] ratios of 0.5 to 8.0. The 2p parameterization of Carlton et al. (2010) was based on all seven data points and was categorized as relevant for high-NO_x conditions; whereas the VBS parameterization of Pye et al. (2010) was based on four of the seven data points, with ΔHC [ppbC] / $NO_{x\,initial}$ [ppb] > 3, and was categorized as relevant for low-NO_x conditions. As shown in Fig. 4a, b the two parameterizations produced quantitatively similar results. These results are consistent with the Griffin et al. (1999) data from which no clear trend as a function of VOC / NO_x ratio was observed. The VOC / NO_x ratios span a much smaller range than that of Ng et al. (2007a), in which the high- and intermediate-NO_x experiments all had ΔHC [ppbC] / $NO_{x\,initial}$ [ppb] < 1 and the low-NO_x experiments > 50; in addition, for all but one experiment (ΔHC [ppbC] / $NO_{x\,initial}$ [ppb] $= 8$) the Griffin et al. (1999) conditions would be classified as high-NO_x based on Presto et al. (2005). Somewhat surprisingly, the clear NO_x-dependency observed by Ng et al. (2007a) over all mass loadings ($M_o = 20$–$214\,\mu g\,m^{-3}$) is no longer observable at the lowest M_o (Fig. 4a, b). Instead there appears to be a greater dependence of SOA yields on the specific sesquiterpene precursor than on VOC / NO_x ratios (see Supplement Fig. S3).

Without the availability of additional data on the NO_x-dependency of SOA formation from different sesquiterpene precursors, the default CMAQv.4.7.1 parameters for sesquiterpenes were retained as the best available for high-NO_x conditions and it was concluded that there were insufficient data to support the derivation and/or use of low-NO_x sesquiterpene parameters. The CMAQ parameters however are not physically realistic, as they indicate a relatively high increase in the mass of the condensing compounds relative to the precursor ($\alpha \approx 1.5$) without a substantial decrease in volatility (unless it is assumed that the sesquiterpene SOA is dominated by highly oxidized sesquiterpene

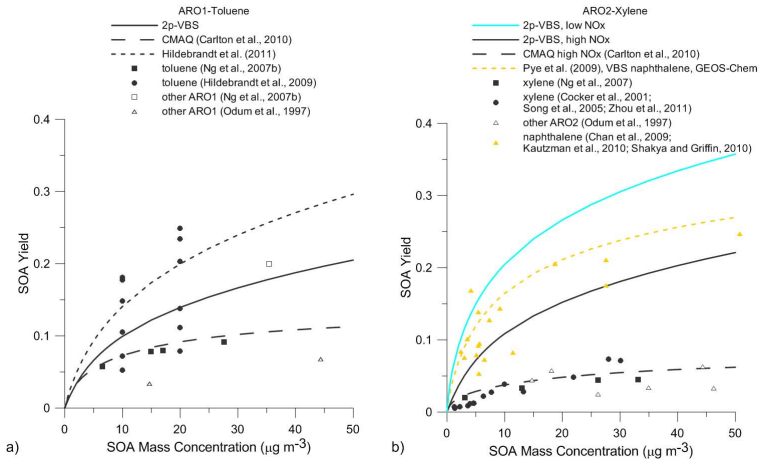

Fig. 5. Evaluation of 2p and 2p-VBS parameterizations for lumped aromatics. **(a)** ARO1/toluene theoretical yield curve (SOA yield vs. SOA mass concentration); **(b)** ARO2/xylene theoretical yield curve.

fragments). This is a consequence of the system of least-squares fitting equations being underdetermined, and thus the derived α and C^* values are non-unique. The single lumped sesquiterpene oxidation product is relatively volatile ($C^* = 25\,\mu g\,m^{-3}$) compared to the lower volatility lumped product of isoprene ($C^* = 0.6\,\mu g\,m^{-3}$) and lumped monoterpenes (2p-VBS, $C^* = 6\,\mu g\,m^{-3}$). Different combinations of derived α and C^* values would produce significantly different results when used in CTMs. In the case of sesquiterpenes, the published C^* value resulted in a calculated SOA yield of $\sim 20\,\%$ at $M_o = 5\,\mu g\,m^{-3}$; this is in contrast to the reported SOA yields of 40–60 % (for $M_o = 10$–$20\,\mu g\,m^{-3}$) shown in Fig. 4. A test set of parameters, more in accord with the monoterpene parameters, reproduced the observed chamber data reasonably well and resulted in a calculated SOA yield of $\sim 45\,\%$ at $M_o = 5\,\mu g\,m^{-3}$. This finding supports the need for additional constraints, chamber data, on sesquiterpene+oxidant systems.

3.2 Anthropogenic precursor parameters

In Figs. 5 and 6, theoretical yield curves (SOA yield vs. M_o) are shown for each of the anthropogenic precursors: lumped high-yield (refers to yield in the gas phase) aromatics (ARO1 in SAPRC, includes toluene), lumped low-yield aromatics (ARO2 in SAPRC, includes xylene), and lumped alkanes (ALK5 in SAPRC). The anthropogenic 2p, VBS, and 2p-VBS parameters were evaluated for high-NO_x conditions only.

3.2.1 Toluene/ARO1 parameters

For toluene/ARO1, the calculated SOA yields were consistent with the data on which each of the parameterizations were based (Fig. 5a). Hildebrandt et al. (2009) reported a range of SOA yields that were highly sensitive to experimental conditions such as UV intensity, temperature, and NO_x levels. For comparable temperatures, the reported SOA yields of Hildebrandt et al. (2009) are higher than those of Ng et al. (2007b); the latter of which were used to derive the 2p parameters in CMAQ (Carlton et al., 2010). Hildebrandt et al. (2009) described the likely reasons for these discrepancies: temperature differences during the experiments (slightly higher in Ng et al., 2007b; less variable in Hildebrandt et al., 2009), differences in NO_2 / NO ratios (NO_2 dominated Hildebrandt et al., 2009; a more atmospherically relevant NO_2 / NO mix in Ng et al., 2007b), and corrections made for vapor loses to walls in Hildebrandt et al. (2009). The Tsimpidi et al. (2010) parameters used to derive the 2p-VBS parameters were based on the data of Ng et al. (2007b) and Hildebrandt et al. (2009), and best represented the middle point of these two datasets (see Fig. 5a). The 2p-VBS parameters for toluene/ARO1 under high-NO_x conditions were thus chosen for the CMAQ simulations.

3.2.2 Xylene/ARO2 parameters

The lumped aromatics category ARO2 in SAPRC07 (Carter, 2010) contains xylenes, as well as the PAH naphthalene. In Fig. 5b, chamber data using naphthalene precursors (Chan et al., 2009; Kautzman et al., 2010; Shakya and Griffin, 2010) were differentiated from chamber data using xylene (Cocker et al., 2001b; Song et al., 2005; Ng et al., 2007b; Zhou et al., 2011) and "other" ARO2 precursors, e.g., methyl- and ethylbenzenes (Odum et al., 1997). There were significant differences in yields among these ARO2 precursors, particularly between naphthalene and xylene/"other". These differences were reflected in the predicted SOA yields using the naphthalene VBS parameters of Pye et al. (2010), based on the chamber data of Chan et al. (2009), and the xylene 2p parameters of Carlton et al. (2010), based on the chamber data of Ng et al. (2007b). Each of these parameterizations represents

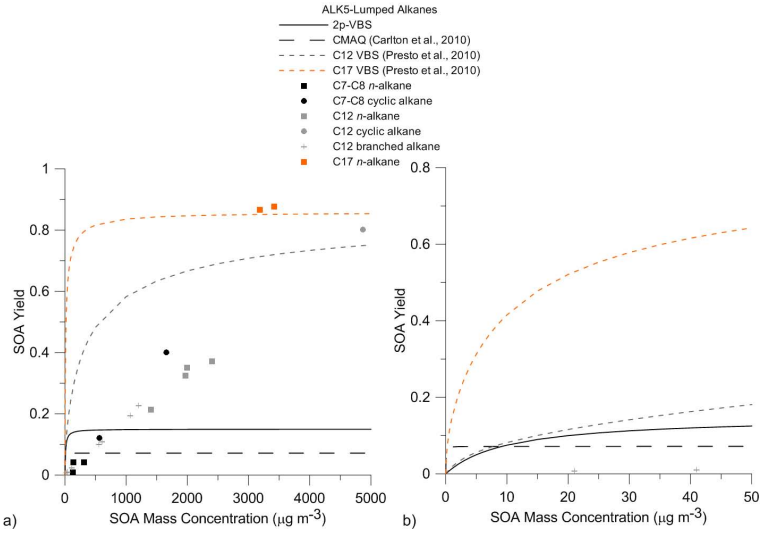

Fig. 6. Evaluation of 2p and 2p-VBS parameterizations for lumped alkanes (≥ C6). Theoretical yield curve (SOA yield vs. SOA mass concentration) for M_o up to 5000 μg m^{-3} **(a)** and M_o up to 50 μg m^{-3} **(b)**; data from Lim and Ziemann (2009).

the available data well, with the caveat that neither parameterization is appropriate for naphthalene *and* xylenes/other lumped ARO2 compounds. The high-NO_x naphthalene VBS parameters of Pye et al. (2010) were used to obtain 2p-VBS parameters, which are provided in Table 2. The naphthalene 2p-VBS parameters were not used in the CMAQ simulations because naphthalene is not treated explicitly in the SAPRC gas-phase chemical mechanism but is lumped with xylene.

The high NO_x ARO2 VBS parameters of Lane et al. (2008a)/Tsimpidi et al. (2010), from which the 2p-VBS parameters were derived, were calculated from the low NO_x ARO2 VBS parameters (Lane et al., 2008b) based on the chamber data of Ng et al. (2007b), by applying a M_o-dependent yield correction based on the α-pinene parameterizations of Pathak et al. (2007a). This approach led to a significant overestimation of SOA formation from xylene and other ARO2 aromatics (excluding naphthalene). Thus, the default CMAQ parameters for ARO2 under high-NO_x conditions were retained as the best available.

3.2.3 Alkane/ALK5 parameters

The lumped alkane species ALK5 includes C6 and higher cycloalkanes, C7 and higher *n*-alkanes, and C8 and higher branched alkanes. From an emissions perspective, the lumped ALK5 species is largely representative of a ∼C8 alkane (e.g., Carlton et al., 2010; Pye and Pouliot, 2012). The CMAQ ALK5 parameters are from Pandis et al. (1992)/Strader et al. (1999), based on the chamber experiments of Grosjean and Seinfeld (1989). They roughly represent SOA formation from C8–C10 *n*-alkanes as measured by Grosjean and Seinfeld (1989). The VBS parameters (Lane et al., 2008b; Tsimpidi et al., 2010) used to obtain the 2p-VBS parameters were based on chamber data of Wang et al. (1992), Takekawa et al. (2003), and Lim and Ziemann (2005) for C8-C15 *n*-alkanes and methylcylcohexane (Wang et al., 1992). Due to limited data availability, both Pandis et al. (1992) and Lane et al. (2008b) derived only one-product fits for this class of lumped alkanes. Calculated SOA yields with the CMAQ 2p parameters (Carlton et al., 2010) and 2p-VBS parameters were compared with chamber data from Lim and Ziemann (2009) for linear and cyclic C8 alkanes (Fig. 6). The default CMAQ parameters were in good agreement with that data for linear C8 alkanes, though may overestimate SOA at lower M_o (Fig. 6b). The 2p-VBS parameters resulted in higher SOA yields at higher ΔHC levels and M_o. This likely was due to the inclusion of cyclic alkane data in the fitting. Lim and Ziemann (2009) demonstrated that alkane SOA yields followed the trend: cyclic alkanes > linear alkanes > branched alkanes; furthermore within each class, SOA yields increased with carbon number.

In addition to 2p and 2p-VBS parameters, VBS parameters from Presto et al. (2010) were compared with the data of Lim and Ziemann (2009) (Fig. 6). Presto et al. (2010) derived VBS parameters for C12-C17 *n*-alkanes, based on *n*-heptadecane data (2p-VBS parameters based on Presto et al. (2010) are provided in Table 2). The theoretical yield curves showed an increase in SOA yield as a function of carbon number, as observed by Lim and Ziemann (2009). At high M_o, the calculated SOA yields were higher than the reported yields of Lim and Ziemann (2009), particularly for the C12 alkanes; however, the experiments were conducted over very different M_o ranges with no overlapping data points and thus, the yields may not be directly comparable. At low M_o (Fig. 6b), there are no data points for evaluation other than those from which the parameterization of Presto et al. (2010) was derived (not shown). Based

on current emissions inventories and the results of Presto et al. (2010), the 2p-VBS parameters were chosen the best available.

The SOA yields from cyclic and C12 and higher *n*-alkanes (Fig. 6) and naphthalene (Fig. 5) were significantly underestimated by the default 2p parameters for the volatile SOA precursors with which they are lumped (cyclic and > C12 alkanes with ALK5 and naphthalene with ARO2) in the gas-phase chemical mechanism SAPRC07 (Carter, 2010). If emissions of such compounds are indeed sufficient to contribute measurably to SOA, as indicated by ambient observations (alkanes: Liu et al., 2011; Russell et al., 2011; de Gouw et al., 2011; naphthalene: Chan et al., 2009; Shakya and Griffin, 2010; Zhang and Ying, 2012), separation of the VOCs with intermediate to low volatility from VOCs in the gas-phase and aerosol models likely will result in more accurate SOA predictions. Pye and Pouliot (2012) recently reported on the explicit treatment of C6–C19 alkanes and PAHs, represented by naphthalene, in CMAQv.5.0. They concluded that C6–C19 alkanes and PAHs could represent 20–30 % of SOA formation (up to 50 ng m^{-3}) with highest contributions in winter, using current emissions inventories. Though similar modification of SAPRC07 and CMAQv4.7.1 was outside the scope of this study, it is recommended that SOA formation by cyclic alkanes, $\geq$ C12 *n*-alkanes and naphthalene be treated independently in future model applications.

3.3 CMAQ model simulations

The base case CMAQ predictions for total SOA, averaged over 15–31 July 2006 are shown in Fig. 7. In regions with the highest predicted concentrations of anthropogenic SOA (up to 1 µg m^{-3}), a net decrease in anthropogenic SOA (up to 20 %) was predicted (figure not shown); the use of best available parameters for ARO1/toluene (2p-VBS) resulted in a slight increase in predicted SOA mass while the use of best available parameters for ALK5 (2p-VBS) resulted in a slight decrease. In regions with the highest predicted concentrations of biogenic SOA (1–2 µg m^{-3} in northern California, southern Oregon and Southeastern US), the predicted increase in total SOA mass was significant, ~ 10–15 % for high-NO_x conditions and up to ~ 200 % (~ 3 µg m^{-3}) for low-NO_x conditions (see Fig. 8). The increase in total SOA was largely a consequence of an increase in biogenic SOA (see Supplement Fig. S4) attributed to the use of the 2p-VBS parameters for lumped monoterpenes. The predicted increases in total SOA correspond to increases in $PM_{2.5}$ of up to 7 % and 55 % for the high- and low-NO_x conditions, respectively, in Western US where $PM_{2.5}$ concentrations in the base case were ~ 2 µg m^{-3}. The 2p-VBS fitting resulted in a 2-fold decrease in the C^*_1 value for lumped monoterpenes (high NO_x), from $C^*_1 = 14.8$ µg m^{-3} (default) to $C^*_1 = 6.3$ µg m^{-3}, which increased the predicted contribution of traditional monoterpene SOA (excluding oligomerization) to total SOA by ~ 10 % in the Southeastern US (from

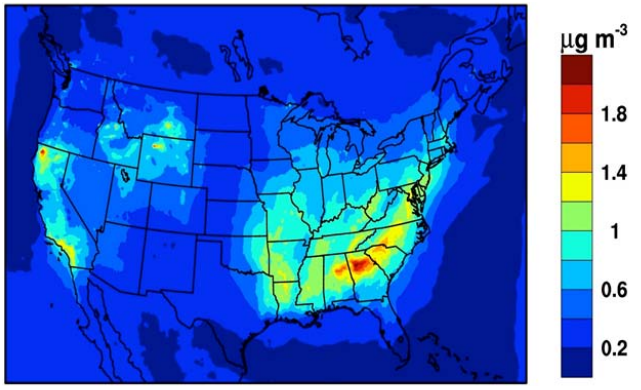

Fig. 7. Total SOA averaged over 15–31 July 2006 for the base case simulation (using default CMAQ parameters).

15–30 % in base case, figure not shown). Under low-NO_x conditions, that contribution was increased by ~ 20–30 % in the Southeastern US (figure not shown).

Figure 9 shows the fraction of RO_2 reacting with NO as compared to that reacting with HO_2, and thus the fractional weighting of high- vs. low-NO_x parameters, illustrating the relative importance of high- vs. low-NO_x pathways in the CMAQ simulations. As noted previously, this fractional weighting is considered in CMAQv.4.7.1 for anthropogenic precursors only, therefore the sensitivity simulations performed here using the high- and low-NO_x 2p-VBS monoterpene parameters indicate the range of SOA that can be formed for the limiting assumptions. It can be seen in Fig. 9 that based on current treatment, low-NO_x pathways and therefore low-NO_x parameters are relevant for SOA formation in many regions of the US.

In Fig. 10, model-based secondary organic carbon (SOC) mass concentrations are compared with observationally-based SOC concentrations. Observationally-based SOC concentrations were calculated according to the method of Yu et al. (2007) using measured organic carbon (OC) and elemental carbon (EC) data from 155 IMPROVE sites. The sites were grouped into six regions: West Pacific, West, Central, Midwest, Northeast, and Southeast; 115 of the 155 sites are in locations where $\geq$ 50 % of RO_2 was predicted to react with HO_2 (i.e., low-NO_x pathway; see Fig. 9). For all three cases, the model- and measurement-based trends in predicted SOC mass concentration follow a similar pattern from region to region, except for the Midwest. For all regions, model-based SOC mass concentrations were in better agreement with measurement-based SOC using the best available parameters, particularly for the low-NO_x case. Averaged over all sites, the percent bias improved from −63 % to −15 % from the base case to the best available low-NO_x case. This is consistent with the higher predicted SOA yields at low M_o and better agreement with chamber data achieved by the best available parameters in the parameter comparisons. SOC mass still was significantly underpredicted in the

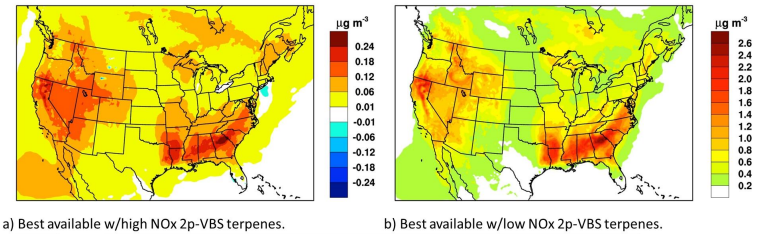

Fig. 8. Difference in total SOA averaged over 15–31 July 2006 between the best available parameter simulation and the base case CMAQ simulation: using the high NO_x 2p-VBS parameters for lumped monoterpenes **(a)**, and using the low NO_x 2p-VBS parameters for lumped monoterpenes **(b)**.

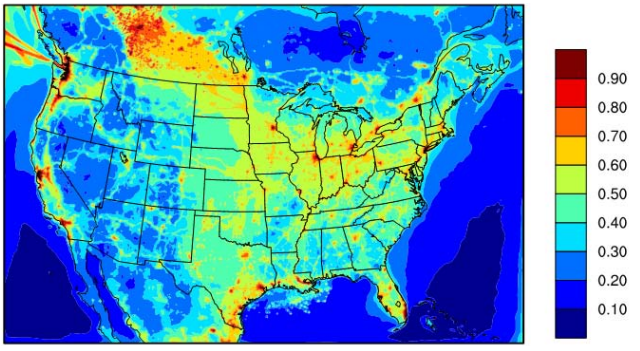

Fig. 9. The fraction of RO_2 reacting with NO (vs. HO_2), indicating the relative importance of high- vs. low-NO_x pathways, respectively, predicted in the CMAQ simulations averaged over the simulation period, 15–31 July 2006.

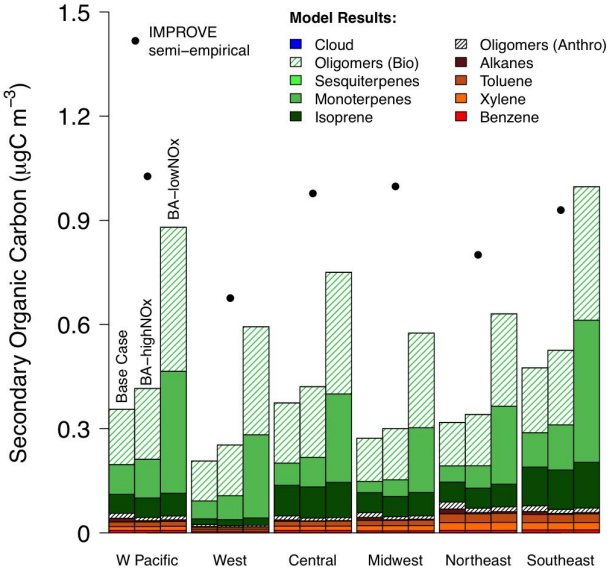

Fig. 10. Regional comparison of model-based (base case and best available high- and low-NO_x cases) and observationally-based secondary organic carbon (SOC) mass concentrations. Observationally-based SOC concentrations were calculated from data averaged over the simulation period from 155 IMPROVE sites.

Midwest, Central and Northeast regions, where the percent bias were −43 %, −23 % and −21 % respectively, for the best available low-NO_x case, suggesting "missing" anthropogenic source(s) and/or other pathway(s).

4 Conclusions

The linkages between experimental conditions, parameter optimization, and predictions of SOA were explored here by: (1) comparing calculated SOA yields and mass concentrations using 2p, VBS, and newly-developed 2p-VBS parameters with a comprehensive list of published smog chamber data for common volatile SOA precursor species; (2) selecting a set of "best available" (BA) parameters defined by best agreement with published chamber data; and (3) analyzing CMAQv4.7.1 model output for the default (base case) and selected sensitivity (BA-highNO_x and BA-lowNO_x) simulations. With regard to parameter fitting, VBS parameterizations may be more robust and less likely to underestimate SOA formation at atmospherically relevant M_o ranges when data are sparse. However, their use is not justified when the underlying data are limited or event absent, especially at low, atmospherically relevant ΔHC and M_o. Extrapolating from high- to low-NO_x conditions, and vice versa, does not produce reliable parameters, particularly when further extrapolating across precursors: data are required for each precursor under a range of NO_x levels (NO_2 / NO ratios). For the common SOA precursors treated in the 2p framework, data gaps are most significant for photo-oxidation of monoterpenes and sesquiterpenes under a range of $HO_2 : NO : NO_2$ levels and for alkanes at low M_o.

While only SOA formation in the traditional view was considered, VOC oxidation followed by condensation of semi-volatile oxidation products, some insight was gained on intermediate to low volatility SOA precursors. The SOA yields from naphthalene and C12 and higher *n*-alkanes, which are currently lumped with VOCs in the gas-phase chemical mechanism SAPRC07 (Carter, 2010), were significantly underestimated by the default 2p parameters. 2p-VBS parameters are provided for these precursors, as well

as POA, though the current SAPRC07/CMAQv4.7.1 configuration did not allow for their evaluation in the context of chemical transport modeling.

Recognizing that many important processes currently are not treated in the CMAQ SOA model (e.g., oxidation of intermediate to low volatility organic compounds, partitioning of POA, and kinetically controlled partitioning), the use of the selected best available parameters in CMAQ nonetheless significantly improved the agreement between model- and measurement-based SOC mass concentrations. More importantly, as demonstrated, the choice of model parameters will impact source-attribution analyses, as well as spatial and temporal distributions of modeled SOA (through the physicochemical properties of SOA they represent), which may adversely affect the accuracy of air quality and climate predictions from CTMs that rely on parameterizations of chamber experiments. In addition to the implementation of more advanced representations of important gas- and particle-phase processes in CMAQ, better representation of "first generation" SOA formation is also needed. Development and application of the 2p-VBS parameters for ALK5, toluene, and particularly monoterpenes, advances that goal within the 2p modeling framework; however, critical data gaps exist for many of the SOA precursors under atmospherically relevant conditions, currently limiting the progress that can be made with chamber data fitting approaches.

Supplementary material related to this article is available online at http://www.atmos-chem-phys.net/13/12073/2013/acp-13-12073-2013-supplement.pdf.

Acknowledgements. The authors would like to thank K. Baker for his help with the CMAQ files. Funding for this work was provided in part by Research and Sponsored Projects and the Institute of Sustainable Solutions at Portland State University.

Edited by: J. H. Seinfeld

References

Aumont, B., Szopa, S., and Madronich, S.: Modelling the evolution of organic carbon during its gas-phase tropospheric oxidation: development of an explicit model based on a self generating approach, Atmos. Chem. Phys., 5, 2497–2517, doi:10.5194/acp-5-2497-2005, 2005.

Barsanti, K. C., Smith, J. N., and Pankow, J. F.: Application of the np plus mP modeling approach for simulating secondary organic particulate matter formation from alpha-pinene oxidation, Atmos. Environ., 45, 6812–6819, doi:10.1016/j.atmosenv.2011.01.038, 2011.

Byun, D. and Schere, K. L.: Review of the governing equations, computational algorithms, and other components of the models-3 Community Multiscale Air Quality (CMAQ) modeling system, Appl. Mech. Rev., 59, 51–77, doi:10.1115/1.2128636, 2006.

Camredon, M., Hamilton, J. F., Alam, M. S., Wyche, K. P., Carr, T., White, I. R., Monks, P. S., Rickard, A. R., and Bloss, W. J.: Distribution of gaseous and particulate organic composition during dark α-pinene ozonolysis, Atmos. Chem. Phys., 10, 2893–2917, doi:10.5194/acp-10-2893-2010, 2010.

Cappa, C. D. and Wilson, K. R.: Evolution of organic aerosol mass spectra upon heating: implications for OA phase and partitioning behavior, Atmos. Chem. Phys., 11, 1895–1911, doi:10.5194/acp-11-1895-2011, 2011.

Carlton, A. G., Wiedinmyer, C., and Kroll, J. H.: A review of Secondary Organic Aerosol (SOA) formation from isoprene, Atmos. Chem. Phys., 9, 4987–5005, doi:10.5194/acp-9-4987-2009, 2009.

Carlton, A. G., Bhave, P. V., Napelenok, S. L., Edney, E. D., Sarwar, G., Pinder, R. W., Pouliot, G. A., and Houyoux, M.: Model Representation of Secondary Organic Aerosol in CMAQv4.7, Environ. Sci. Technol., 44, 8553–8560, doi:10.1021/es100636q, 2010.

Carter, W. P. L.: Development of the SAPRC-07 chemical mechanism, Atmos. Environ., 44, 5324–5335, doi:10.1016/j.atmosenv.2010.01.026, 2010.

Chan, A. W. H., Kautzman, K. E., Chhabra, P. S., Surratt, J. D., Chan, M. N., Crounse, J. D., Kürten, A., Wennberg, P. O., Flagan, R. C., and Seinfeld, J. H.: Secondary organic aerosol formation from photooxidation of naphthalene and alkylnaphthalenes: implications for oxidation of intermediate volatility organic compounds (IVOCs), Atmos. Chem. Phys., 9, 3049–3060, doi:10.5194/acp-9-3049-2009, 2009.

Chan, A. W. H., Chan, M. N., Surratt, J. D., Chhabra, P. S., Loza, C. L., Crounse, J. D., Yee, L. D., Flagan, R. C., Wennberg, P. O., and Seinfeld, J. H.: Role of aldehyde chemistry and NO_X concentrations in secondary organic aerosol formation, Atmos. Chem. Phys., 10, 7169–7188, doi:10.5194/acp-10-7169-2010, 2010.

Chhabra, P. S., Flagan, R. C., and Seinfeld, J. H.: Elemental analysis of chamber organic aerosol using an aerodyne high-resolution aerosol mass spectrometer, Atmos. Chem. Phys., 10, 4111–4131, doi:10.5194/acp-10-4111-2010, 2010.

Chung, S. H. and Seinfeld, J. H.: Global distribution and climate forcing of carbonaceous aerosols, J. Geophys. Res.-Atmos., 107, 4407, doi:10.1029/2001jd001397, 2002.

Cocker, D. R., Clegg, S. L., Flagan, R. C., and Seinfeld, J. H.: The effect of water on gas-particle partitioning of secondary organic aerosol. Part I: alpha-pinene/ozone system, Atmos. Environ., 35, 6049–6072, doi:10.1016/s1352-2310(01)00404-6, 2001a.

Cocker, D. R., Mader, B. T., Kalberer, M., Flagan, R. C., and Seinfeld, J. H.: The effect of water on gas-particle partitioning of secondary organic aerosol: II. m-xylene and 1,3,5-trimethylbenzene photooxidation systems, Atmos. Environ., 35, 6073–6085, doi:10.1016/s1352-2310(01)00405-8, 2001b.

de Gouw, J. A., Middlebrook, A. M., Warneke, C., Ahmadov, R., Atlas, E. L., Bahreini, R., Blake, D. R., Brock, C. A., Brioude, J., Fahey, D. W., Fehsenfeld, F. C., Holloway, J. S., Le Henaff, M., Lueb, R. A., McKeen, S. A., Meagher, J. F., Murphy, D. M., Paris, C., Parrish, D. D., Perring, A. E., Pollack, I. B., Ravishankara, A. R., Robinson, A. L., Ryerson, T. B., Schwarz, J. P., Spackman, J. R., Srinivasan, A., and Watts, L. A.: Organic Aerosol Formation Downwind from the Deepwater Horizon Oil

Spill, Science, 331, 1295–1299, doi:10.1126/science.1200320, 2011.

Donahue, N. M., Robinson, A. L., Stanier, C. O., and Pandis, S. N.: Coupled partitioning, dilution, and chemical aging of semivolatile organics, Environ. Sci. Technol., 40, 02635–02643, doi:10.1021/es052297c, 2006.

Goldstein, A. H., Koven, C. D., Heald, C. L., and Fung, I. Y.: Biogenic carbon and anthropogenic pollutants combine to form a cooling haze over the southeastern United States, P. Natl. Acad. Sci. USA, 106, 8835–8840, doi:10.1073/pnas.0904128106, 2009.

Grieshop, A. P., Miracolo, M. A., Donahue, N. M., and Robinson, A. L.: Constraining the Volatility Distribution and Gas-Particle Partitioning of Combustion Aerosols Using Isothermal Dilution and Thermodenuder Measurements, Environ. Sci. Technol., 43, 4750–4756, doi:10.1021/es8032378, 2009.

Griffin, R. J., Cocker, D. R., Flagan, R. C., and Seinfeld, J. H.: Organic aerosol formation from the oxidation of biogenic hydrocarbons, J. Geophys. Res.-Atmos., 104, 3555–3567, 1999.

Grosjean, D. and Seinfeld, J. H.: Parameterization of the formation potential of secondary organic aerosols, Atmos. Environ., 23, 1733–1747, doi:10.1016/0004-6981(89)90058-9, 1989.

Hallquist, M., Wenger, J. C., Baltensperger, U., Rudich, Y., Simpson, D., Claeys, M., Dommen, J., Donahue, N. M., George, C., Goldstein, A. H., Hamilton, J. F., Herrmann, H., Hoffmann, T., Iinuma, Y., Jang, M., Jenkin, M. E., Jimenez, J. L., Kiendler-Scharr, A., Maenhaut, W., McFiggans, G., Mentel, Th. F., Monod, A., Prévôt, A. S. H., Seinfeld, J. H., Surratt, J. D., Szmigielski, R., and Wildt, J.: The formation, properties and impact of secondary organic aerosol: current and emerging issues, Atmos. Chem. Phys., 9, 5155–5236, doi:10.5194/acp-9-5155-2009, 2009.

Haywood, J. and Boucher, O.: Estimates of the direct and indirect radiative forcing due to tropospheric aerosols: A review, Rev. Geophys., 38, 513–543, 2000.

Heald, C. L., Henze, D. K., Horowitz, L. W., Feddema, J., Lamarque, J. F., Guenther, A., Hess, P. G., Vitt, F., Seinfeld, J. H., Goldstein, A. H., and Fung, I.: Predicted change in global secondary organic aerosol concentrations in response to future climate, emissions, and land use change, J. Geophys. Res.-Atmos., 113, D05211, doi:10.1029/2007jd009092, 2008.

Henze, D. K. and Seinfeld, J. H.: Global secondary organic aerosol from isoprene oxidation, Geophys. Res. Lett., 33, L09812, doi:10.1029/2006gl025976, 2006.

Henze, D. K., Seinfeld, J. H., Ng, N. L., Kroll, J. H., Fu, T.-M., Jacob, D. J., and Heald, C. L.: Global modeling of secondary organic aerosol formation from aromatic hydrocarbons: high-vs. low-yield pathways, Atmos. Chem. Phys., 8, 2405–2420, doi:10.5194/acp-8-2405-2008, 2008.

Hildebrandt, L., Donahue, N. M., and Pandis, S. N.: High formation of secondary organic aerosol from the photo-oxidation of toluene, Atmos. Chem. Phys., 9, 2973–2986, doi:10.5194/acp-9-2973-2009, 2009.

Hoffmann, T., Odum, J. R., Bowman, F., Collins, D., Klockow, D., Flagan, R. C., and Seinfeld, J. H.: Formation of organic aerosols from the oxidation of biogenic hydrocarbons, J. Atmos. Chem., 26, 189–222, 1997.

Kautzman, K. E., Surratt, J. D., Chan, M. N., Chan, A. W. H., Hersey, S. P., Chhabra, P. S., Dalleska, N. F., Wennberg, P. O., Flagan, R. C., and Seinfeld, J. H.: Chemical Composition of Gas- and Aerosol-Phase Products from the Photooxidation of Naphthalene, J. Phys. Chem. A, 114, 913–934, doi:10.1021/jp908530s, 2010.

Kleindienst, T. E., Lewandowski, M., Offenberg, J. H., Edney, E. O., Jaoui, M., Zheng, M., Ding, X. A., and Edgerton, E. S.: Contribution of Primary and Secondary Sources to Organic Aerosol and $PM_{2.5}$ at SEARCH Network Sites, J. Air Waste Manage., 60, 1388–1399, doi:10.3155/1047-3289.60.11.1388, 2010.

Kroll, J. H. and Seinfeld, J. H.: Chemistry of secondary organic aerosol: Formation and evolution of low-volatility organics in the atmosphere, Atmos. Environ., 42, 3593–3624, doi:10.1016/j.atmosenv.2008.01.003, 2008.

Kroll, J. H., Ng, N. L., Murphy, S. M., Flagan, R. C., and Seinfeld, J. H.: Secondary organic aerosol formation from isoprene photooxidation under high-NO_x conditions, Geophys. Res. Lett., 32, L18808, doi:10.1029/2005gl023637, 2005.

Kroll, J. H., Ng, N. L., Murphy, S. M., Flagan, R. C., and Seinfeld, J. H.: Secondary organic aerosol formation from isoprene photooxidation, Environ. Sci. Technol., 40, 1869–1877, doi:10.1021/es0524301, 2006.

Lack, D. A., Tie, X. X., Bofinger, N. D., Wiegand, A. N., and Madronich, S.: Seasonal variability of secondary organic aerosol: A global modeling study, J. Geophys. Res.-Atmos., 109, D03203, doi:10.1029/2003jd003418, 2004.

Lane, T. E., Donahue, N. M., and Pandis, S. N.: Effect of NO_x on secondary organic aerosol concentrations, Environ. Sci. Technol., 42, 6022–6027, doi:10.1021/es703225a, 2008a.

Lane, T. E., Donahue, N. M., and Pandis, S. N.: Simulating secondary organic aerosol formation using the volatility basis-set approach in a chemical transport model, Atmos. Environ., 42, 7439–7451, doi:10.1016/j.atmosenv.2008.06.026, 2008b.

Lee-Taylor, J., Madronich, S., Aumont, B., Baker, A., Camredon, M., Hodzic, A., Tyndall, G. S., Apel, E., and Zaveri, R. A.: Explicit modeling of organic chemistry and secondary organic aerosol partitioning for Mexico City and its outflow plume, Atmos. Chem. Phys., 11, 13219–13241, doi:10.5194/acp-11-13219-2011, 2011.

Lim, Y. B. and Ziemann, P. J.: Products and mechanism of secondary organic aerosol formation from reactions of n-alkanes with OH radicals in the presence of NO_x, Environ. Sci. Technol., 39, 9229–9236, doi:10.1021/es051447g, 2005.

Lim, Y. B. and Ziemann, P. J.: Effects of Molecular Structure on Aerosol Yields from OH Radical-Initiated Reactions of Linear, Branched, and Cyclic Alkanes in the Presence of NO_x, Environ. Sci. Technol., 43, 2328–2334, doi:10.1021/es803389s, 2009.

Liu, S., Day, D. A., Shields, J. E., and Russell, L. M.: Ozone-driven daytime formation of secondary organic aerosol containing carboxylic acid groups and alkane groups, Atmos. Chem. Phys., 11, 8321–8341, doi:10.5194/acp-11-8321-2011, 2011.

Myhre, G., Berglen, T. F., Johnsrud, M., Hoyle, C. R., Berntsen, T. K., Christopher, S. A., Fahey, D. W., Isaksen, I. S. A., Jones, T. A., Kahn, R. A., Loeb, N., Quinn, P., Remer, L., Schwarz, J. P., and Yttri, K. E.: Modelled radiative forcing of the direct aerosol effect with multi-observation evaluation, Atmos. Chem. Phys., 9, 1365–1392, doi:10.5194/acp-9-1365-2009, 2009.

Ng, N. L., Kroll, J. H., Keywood, M. D., Bahreini, R., Varutbangkul, V., Flagan, R. C., Seinfeld, J. H., Lee, A., and Goldstein, A. H.: Contribution of first- versus second-generation

products to secondary organic aerosols formed in the oxidation of biogenic hydrocarbons, Environ. Sci. Technol., 40, 2283–2297, doi:10.1021/es052269u, 2006.

Ng, N. L., Chhabra, P. S., Chan, A. W. H., Surratt, J. D., Kroll, J. H., Kwan, A. J., McCabe, D. C., Wennberg, P. O., Sorooshian, A., Murphy, S. M., Dalleska, N. F., Flagan, R. C., and Seinfeld, J. H.: Effect of NO_x level on secondary organic aerosol (SOA) formation from the photooxidation of terpenes, Atmos. Chem. Phys., 7, 5159–5174, doi:10.5194/acp-7-5159-2007, 2007a.

Ng, N. L., Kroll, J. H., Chan, A. W. H., Chhabra, P. S., Flagan, R. C., and Seinfeld, J. H.: Secondary organic aerosol formation from *m*-xylene, toluene, and benzene, Atmos. Chem. Phys., 7, 3909–3922, doi:10.5194/acp-7-3909-2007, 2007b.

Odum, J. R., Hoffmann, T., Bowman, F., Collins, D., Flagan, R. C., and Seinfeld, J. H.: Gas/particle partitioning and secondary organic aerosol yields, Environ. Sci. Technol., 30, 2580–2585, 1996.

Odum, J. R., Jungkamp, T. P. W., Griffin, R. J., Forstner, H. J. L., Flagan, R. C., and Seinfeld, J. H.: Aromatics, reformulated gasoline, and atmospheric organic aerosol formation, Environ. Sci. Technol., 31, 1890–1897, doi:10.1021/es960535l, 1997.

Pandis, S. N., Paulson, S. E., Seinfeld, J. H., and Flagan, R. C.: Aerosol formation in the photooxidation of isoprene and beta-pinene, Atmos. Environ. Part A-Gen., 25, 997–1008, doi:10.1016/0960-1686(91)90141-s, 1991.

Pandis, S. N., Harley, R. A., Cass, G. R., and Seinfeld, J. H.: Secondary organic aerosol formation and transport, Atmos. Environ. Part A-Gen., 26, 2269–2282, doi:10.1016/0960-1686(92)90358-r, 1992.

Pankow, J. F.: An absorption-model of gas-particle partitioning of organic-compounds in the atmosphere, Atmos. Environ., 28, 185–188, 1994a.

Pankow, J. F.: An absorption-model of the gas aerosol partitioning involved in the formation of secondary organic aerosol, Atmos. Environ., 28, 189–193, 1994b.

Pankow, J. F. and Barsanti, K. C.: The carbon number-polarity grid: A means to manage the complexity of the mix of organic compounds when modeling atmospheric organic particulate matter, Atmos. Environ., 43, 2829–2835, doi:10.1016/j.atmosenv.2008.12.050, 2009.

Park, R. J., Kim, M. J., Jeong, J. I., Youn, D., and Kim, S.: A contribution of brown carbon aerosol to the aerosol light absorption and its radiative forcing in East Asia, Atmos. Environ., 44, 1414–1421, doi:10.1016/j.atmosenv.2010.01.042, 2010.

Pathak, R. K., Presto, A. A., Lane, T. E., Stanier, C. O., Donahue, N. M., and Pandis, S. N.: Ozonolysis of α-pinene: parameterization of secondary organic aerosol mass fraction, Atmos. Chem. Phys., 7, 3811–3821, doi:10.5194/acp-7-3811-2007, 2007a.

Pathak, R. K., Stanier, C. O., Donahue, N. M., and Pandis, S. N.: Ozonolysis of alpha-pinene at atmospherically relevant concentrations: Temperature dependence of aerosol mass fractions (yields), J. Geophys. Res.-Atmos., 112, D03201, doi:10.1029/2006jd007436, 2007b.

Perraud, V., Bruns, E. A, Ezell, M. J., Johnson, S. N., Yu, Y., Alexander, M. L.,Zelenyuk, A., Imre, D., Chang, W. L, Dabdub, D., Pankow, J. F., and Finlayson-Pitts, B. J.: Nonequilibrium atmospheric secondary organic aerosol formation and growth, P. Natl. Acad. Sci. USA, 109, 2836–2841, 2012.

Pope, C. A.: Mortality effects of longer term exposures to fine particulate air pollution: Review of recent epidemiological evidence, Inhal. Toxicol., 19, 33–38, doi:10.1080/08958370701492961, 2007.

Presto, A. A. and Donahue, N. M.: Investigation of alpha-pinene plus ozone secondary organic aerosol formation at low total aerosol mass, Environ. Sci. Technol., 40, 3536–3543, doi:10.1021/es052203z, 2006.

Presto, A. A., Hartz, K. E. H., and Donahue, N. M.: Secondary organic aerosol production from terpene ozonolysis. 2. Effect of NO_x concentration, Environ. Sci. Technol., 39, 7046–7054, doi:10.1021/es050400s, 2005.

Presto, A. A., Miracolo, M. A., Donahue, N. M., and Robinson, A. L.: Secondary Organic Aerosol Formation from High-NO_x Photo-Oxidation of Low Volatility Precursors: n-Alkanes, Environ. Sci. Technol., 44, 2029–2034, doi:10.1021/es903712r, 2010.

Pye, H. O. T. and Pouliot, G. A.: Modeling the Role of Alkanes, Polycyclic Aromatic Hydrocarbons, and Their Oligomers in Secondary Organic Aerosol Formation, Environ. Sci. Technol., 46, 6041–6047, doi:10.1021/es300409w, 2012.

Pye, H. O. T., Chan, A. W. H., Barkley, M. P., and Seinfeld, J. H.: Global modeling of organic aerosol: the importance of reactive nitrogen (NO_x and NO_3), Atmos. Chem. Phys., 10, 11261–11276, doi:10.5194/acp-10-11261-2010, 2010.

Russell, L. M., Bahadur, R., and Ziemann, P. J.: Identifying organic aerosol sources by comparing functional group composition in chamber and atmospheric particles, P. Natl. Acad. Sci. USA, 108, 3516–3521, doi:10.1073/pnas.1006461108, 2011.

Saleh, R., Donahue, N. M., and Robinson, A. L.: Time scales for gas-particle partitioning equilibration of secondary organic aerosol formed from alpha-pinene ozonolysis, Environ. Sci. Technol., 47, 5588–5594, 2013.

Shakya, K. M. and Griffin, R. J.: Secondary Organic Aerosol from Photooxidation of Polycyclic Aromatic Hydrocarbons, Environ. Sci. Technol., 44, 8134–8139, doi:10.1021/es1019417, 2010.

Shilling, J. E., Chen, Q., King, S. M., Rosenoern, T., Kroll, J. H., Worsnop, D. R., McKinney, K. A., and Martin, S. T.: Particle mass yield in secondary organic aerosol formed by the dark ozonolysis of α-pinene, Atmos. Chem. Phys., 8, 2073–2088, doi:10.5194/acp-8-2073-2008, 2008.

Shiraiwa, M. and Seinfeld, J. H.: Equilibration timescale of atmospheric secondary organic aerosol partitioning, Geophys. Res. Lett., 39, L24801, doi:10.1029/2012GL054008, 2012.

Shrivastava, M. K., Lane, T. E., Donahue, N. M., Pandis, S. N., and Robinson, A. L.: Effects of gas particle partitioning and aging of primary emissions on urban and regional organic aerosol concentrations, J. Geophys. Res.-Atmos., 113, D18301, doi:10.1029/2007jd009735, 2008.

Shrivastava, M., Fast, J., Easter, R., Gustafson Jr., W. I., Zaveri, R. A., Jimenez, J. L., Saide, P., and Hodzic, A.: Modeling organic aerosols in a megacity: comparison of simple and complex representations of the volatility basis set approach, Atmos. Chem. Phys., 11, 6639–6662, doi:10.5194/acp-11-6639-2011, 2011.

Song, C., Na, K. S., and Cocker, D. R.: Impact of the hydrocarbon to NO_x ratio on secondary organic aerosol formation, Environ. Sci. Technol., 39, 3143–3149, doi:10.1021/es0493244, 2005.

Song, C., Na, K., Warren, B., Malloy, Q., and Cocker, D. R.: Secondary organic aerosol formation from the photooxidation

of p- and o-xylene, Environ. Sci. Technol., 41, 7403–7408, doi:10.1021/es0621041, 2007.

Spracklen, D. V., Jimenez, J. L., Carslaw, K. S., Worsnop, D. R., Evans, M. J., Mann, G. W., Zhang, Q., Canagaratna, M. R., Allan, J., Coe, H., McFiggans, G., Rap, A., and Forster, P.: Aerosol mass spectrometer constraint on the global secondary organic aerosol budget, Atmos. Chem. Phys., 11, 12109–12136, doi:10.5194/acp-11-12109-2011, 2011.

Strader, R., Lurmann, F., and Pandis, S. N.: Evaluation of secondary organic aerosol formation in winter, Atmos. Environ., 33, 4849–4863, doi:10.1016/s1352-2310(99)00310-6, 1999.

Surratt, J. D., Chan, A. W. H., Eddingsaas, N. C., Chan, M. N., Loza, C. L., Kwan, A. J., Hersey, S. P., Flagan, R. C., Wennberg, P. O., and Seinfeld, J. H.: Reactive intermediates revealed in secondary organic aerosol formation from isoprene, P. Natl. Acad. Sci. USA, 107, 6640–6645, doi:10.1073/pnas.0911114107, 2010.

Takekawa, H., Minoura, H., and Yamazaki, S.: Temperature dependence of secondary organic aerosol formation by photo-oxidation of hydrocarbons, Atmos. Environ., 37, 3413–3424, doi:10.1016/s1352-2310(03)00359-5, 2003.

Tsimpidi, A. P., Karydis, V. A., Zavala, M., Lei, W., Molina, L., Ulbrich, I. M., Jimenez, J. L., and Pandis, S. N.: Evaluation of the volatility basis-set approach for the simulation of organic aerosol formation in the Mexico City metropolitan area, Atmos. Chem. Phys., 10, 525–546, doi:10.5194/acp-10-525-2010, 2010.

Tsimpidi, A. P., Karydis, V. A., Zavala, M., Lei, W., Bei, N., Molina, L., and Pandis, S. N.: Sources and production of organic aerosol in Mexico City: insights from the combination of a chemical transport model (PMCAMx-2008) and measurements during MILAGRO, Atmos. Chem. Phys., 11, 5153–5168, doi:10.5194/acp-11-5153-2011, 2011.

Vaden, T. D., Imre, D., Beranek, J., Shrivastava, M., and Zelenyuk, A.: Evaporation kinetics and phase of laboratory and ambient secondary organic aerosol, P. Natl. Acad. Sci. USA, 108, 2190–2195, 2011.

Virtanen, A., Joutsensaari, J., Koop, T., Kannosto, J., Yli-Pirila, P., Leskinen, J., Makela, J. M., Holopainen, J. K., Poeschl, U., Kulmala, M., Worsnop, D. R., and Laaksonen, A.: An amorphous solid state of biogenic secondary organic aerosol particles, Nature, 467, 824–827, 2010.

Updyke, K. M., Nguyen, T. B., and Nizkorodov, S. A.: Formation of brown carbon via reactions of ammonia with secondary organic aerosols from biogenic and anthropogenic precursors, Atmos. Environ., 63, 22–31, doi:10.1016/j.atmosenv.2012.09.012, 2012.

Wang, S. C., Paulson, S. E., Grosjean, D., Flagan, R. C., and Seinfeld, J. H.: Aerosol formation and growth in atmospheric organic NO_X systems .1. outdoor smog chamber studies of C-7-hydrocarbons and C-8-hydrocarbons, Atmos. Environ. Part A-Gen., 26, 403–420, doi:10.1016/0960-1686(92)90326-g, 1992.

Xie, Y., Paulot, F., Carter, W. P. L., Nolte, C. G., Luecken, D. J., Hutzell, W. T., Wennberg, P. O., Cohen, R. C., and Pinder, R. W.: Understanding the impact of recent advances in isoprene photooxidation on simulations of regional air quality, Atmos. Chem. Phys., 13, 8439–8455, doi:10.5194/acp-13-8439-2013, 2013.

Yu, S., Bhave, P. V., Dennis, R. L., and Mathur, R.: Seasonal and regional variations of primary and secondary organic aerosol over the continental United States: Semi-empirical estimates and model evaluation, Environ. Sci. Technol., 41, 4690–4697, 2007.

Yu, J. Z., Cocker, D. R., Griffin, R. J., Flagan, R. C., and Seinfeld, J. H.: Gas-phase ozone oxidation of monoterpenes: Gaseous and particulate products, J. Atmos. Chem., 34, 207–258, 1999.

Zhang, H. L. and Ying, Q.: Secondary organic aerosol from polycyclic aromatic hydrocarbons in Southeast Texas, Atmos. Environ., 55, 279–287, doi:10.1016/j.atmosenv.2012.03.043, 2012.

Zhou, Y., Zhang, H. F., Parikh, H. M., Chen, E. H., Rattanavaraha, W., Rosen, E. P., Wang, W. X., and Kamens, R. M.: Secondary organic aerosol formation from xylenes and mixtures of toluene and xylenes in an atmospheric urban hydrocarbon mixture: Water and particle seed effects (II), Atmos. Environ., 45, 3882–3890, doi:10.1016/j.atmosenv.2010.12.048, 2011.